

# Parity Breaking in Nematic Tactoids

P Prinsen<sup>†</sup> and P van der Schoot<sup>‡</sup>

<sup>†</sup> Complex Fluids Theory, Faculty of Applied Sciences, Delft University of Technology, P.O. Box 5057, 2600 GB Delft, The Netherlands

<sup>‡</sup> Eindhoven Polymer Laboratories, Eindhoven University of Technology, P.O. Box 513, 5600 MB Eindhoven, The Netherlands

E-mail: p.prinsen@tnw.tudelft.nl

**Abstract.** We theoretically investigate under what conditions the director field in a spindle-shaped nematic droplet or tactoid obtains a twisted, parity-broken structure. By minimizing the sum of the bulk elastic and surface energies, we show that a twisted director field is stable if the twist and bend elastic constants are small enough compared to the splay elastic constant, but only if the droplet volume is larger than some minimum value. We furthermore show that the transition from an untwisted to a twisted director-field structure is a sharp function of the various control parameters. We predict that suspensions of rigid, rod-like particles cannot support droplets with a parity broken structure, whereas they could possibly occur in those of semi-flexible, worm-like particles.

Submitted to: *JPCM*

PACS numbers: 61.30.Pq, 61.30.Dk, 64.70.Md, 82.70.Dd

## 1. Introduction

Tactoids are metastable nematic liquid crystalline droplets suspended in the co-existing isotropic fluid parent phase [1, 2, 3, 4, 5, 6, 7]. They can adopt a variety of shapes and director-field configurations, depending on their size, on their elastic properties and on the degree of anisotropy of the surface tension [8, 9, 10, 11, 12, 13, 14, 15, 16, 17, 18]. Theoretically, small nematic droplets tend to be quite elongated with a director field that is uniform, whereas very large droplets should be more or less spheroidal with a bipolar director field that supports two surface defects called boojums [8]. The transformation of the shape and the director-field configuration of the droplets with increasing size appears to be continuous [9]. It should be noted that tactoids are quite different from the usual polymer dispersed liquid crystals or PDLCs, in which nematic droplets are embedded in a (solid) polymeric matrix. Indeed, in PDLCs the liquid-crystalline droplets have little opportunity to adjust their shape once the polymer matrix has set. Their surface anchoring is usually also fixed by a strongly anisotropic surface tension that is not nearly as small as seems to be the case in tactoids [8, 19].

In 1985, Williams showed theoretically that spherical bipolar droplets can also exhibit a parity-broken, twisted director field without the nematogens needing to be chiral [10]. Twist transitions have in fact also been predicted to occur in other geometries including nematic fluids confined between two concentric spheres [20] and in so-called hybrid nematic layers [21, 22, 23]. In a twisted nematic droplet the director field circles around the main droplet axis as shown in Figure 1. Twisted bipolar droplets have indeed been observed in thermotropic liquid crystals [5, 24, 25]. To our knowledge, they have not been observed in lyotropic liquid crystals—as we shall see, this may be connected with their typical elongated, spindle-like shape.

In this paper, we extend the work of Williams by considering tactoids of finite size, that is, we allow for nematic droplet shapes that are not necessarily spherical, and for director fields that are not truly bipolar. Our aim is to estimate the minimum size for the twisted director field to be stable in relation to the elastic properties of the nematic and the interfacial tension between the co-existing nematic and isotropic phases. To this end, we first, in section 2, write down a phenomenological free energy consisting of the sum of the usual Frank energy of the elastic deformation of the director field, and a surface free energy of the Rapini-Papoular type [26], and discuss the earlier work of Williams.

Next, in section 3, we present our parametrization of the problem, which is based on one that we introduced in previous work, and that allows for (but does not impose) a continuous transformation from a bipolar to a uniform director field, and from a spherical to a highly elongated spindle-like droplet. Here, we add an extra degree of freedom to describe a potentially twisted director field, being the maximum surface twist angle, as parameter. In section 4, we first discuss truly bipolar droplets, which can largely be dealt with analytically, and generalize Williams' result to bipolar droplets of arbitrary aspect ratio. As we shall see, the larger their aspect ratio, the less likely a

twisted director-field configuration. We numerically investigate the more general case of droplets that can optimize their structure within a prescribed class of droplet shape and director-field geometry, in section 5. We find that the transition to a twisted structure, if it occurs, is sharp at a critical dimensionless volume  $v_0$  and that the droplet is twisted for all volumes  $v > v_0$  greater than that. The critical volume  $v_0$  is a complex function of the various elastic constants and of the anisotropic surface tension. We find that for lyotropic liquid crystals the twist transition must occur at droplet volumes three to six orders of magnitude larger than that for thermotropic liquid crystals. This presumably explains why twisted structures have not yet been observed in the former, whereas they have in the latter. Finally, in the last section, section 6, we summarize our conclusions.

## 2. Free Energy

Presuming the bulk free energy describing the thermodynamic stability of a nematic droplet to be independent of its macroscopic structure, the excess free energy  $F$  relevant to the problem in hand may be written as [14]

$$F = F_E + F_S, \quad (1)$$

$$F_E = \frac{1}{2} \int_V d^3\mathbf{r} [K_{11} (\nabla \cdot \mathbf{n})^2 + K_{22} (\mathbf{n} \cdot \nabla \times \mathbf{n})^2 + K_{33} (\mathbf{n} \times (\nabla \times \mathbf{n}))^2], \quad (2)$$

$$F_S = \tau \int_S d^2\mathbf{r} (1 + \omega(\mathbf{q} \cdot \mathbf{n})^2), \quad (3)$$

where the volume integral  $F_E$  accounts for a possible elastic deformation of the director field, and the surface integral  $F_S$  for the interfacial free energy. Here,  $\mathbf{n}(\mathbf{r})$  denotes the director field at position  $\mathbf{r}$ ,  $\mathbf{q} = \mathbf{q}(\mathbf{r})$  is the normal to the droplet surface,  $K_{11}$ ,  $K_{22}$  and  $K_{33}$  are the familiar Frank elastic constants for splay, twist and bend deformations,  $\tau$  is the isotropic interfacial tension and  $\omega \geq 0$  a dimensionless anchoring strength, penalizing a nonplanar alignment of the director field to the interface.

In equation (2), we ignore the contributions of the surface elastic constants  $K_{13}$  and  $K_{24}$ , associated with splay-bend and saddle-splay deformations. The splay-bend contribution we drop for simplicity, because keeping this term would, in principle, require the incorporation of higher order gradients in the director field to keep the problem well posed [27]. We note in passing that Yokoyama recently argued on quite general grounds that  $K_{13}$  should in fact vanish identically [28]. As for the saddle-splay contribution, it merely renormalizes the splay elastic constant  $K_{11}$  [9], at least for twist-free, bispherical director-field configurations, in which case  $K_{11} \rightarrow K_{11} - K_{24}$  [9]. In a twisted bipolar configuration this is no longer strictly accurate but we do not expect that accounting for the splay-bend elasticity would qualitatively affect the stability of the twisted director field for reasons that we discuss in more detail in section 4. It should be stressed that in certain geometries, such as in hybrid nematic cells with a homeotropic alignment on one boundary surface and planar alignment on the other, or in nematic layers with a mutually perpendicular planar alignment on both surfaces, the saddle splay contribution can induce a twist transition [21, 22, 23], so the issue does indeed deserve some attention.

The optimal droplet shape and director-field configuration minimizes equation (1) at constant volume  $V$  of the drop and at constant unit length of the director  $|\mathbf{n}(\mathbf{r})|^2 = 1$ . This highly non-trivial free boundary problem can be simplified considerably in the limit of  $V/\tau K_{ii}\omega \rightarrow \infty$ , because then the droplet is spherical and the director field is aligned tangentially to the interface [9]. Tacitly presuming this limit to hold, Williams showed that for the twisted bipolar configuration to be favored, the elastic constants of the nematic would have to obey the inequality [10]

$$\gamma_{33} \leq \frac{4\pi^2 - 16}{20 - \pi^2}(1 - \gamma_{22}) \approx 2.32(1 - \gamma_{22}), \quad (4)$$

where  $\gamma_{22} \equiv K_{22}/K_{11}$  and  $\gamma_{33} \equiv K_{33}/K_{11}$ . This inequality expresses the circumstance that by adopting a twisted configuration, a droplet can lower its splay energy albeit at the cost of raising its bend and twist energy. Hence, if the bend and twist elastic constants are small enough compared to the splay elastic constant, a twisted configuration can become energetically favorable. Volovik and Lavrentovich were the first to observe a twisted bipolar droplet in a thermotropic nematic liquid crystal [24]. Available experimental data seem to indicate that equation (4) indeed holds [6].

Whilst twisted bipolar drops have been observed in thermotropic nematics, such is as far as we are aware not the case for lyotropic ones. This may, of course, be linked to them not obeying equation (4). Indeed, theoretical calculations show that for hard, rod-like particles,  $\gamma_{22} \approx 1/3$  and  $\gamma_{33} \gtrsim 5$  at least if they are sufficiently slender [29, 30, 35]. These predictions agree with experimental data on aqueous dispersions of tobacco mosaic virus particles that to a first approximation behave like hard rods, with  $\gamma_{22} \approx 0.2 - 0.4$  and  $\gamma_{33} \approx 9 - 17$  [31, 32]. So, it seems that a nematic of rod-like particles interacting via purely repulsive interactions do not obey the Williams inequality, equation (4), and hence should not display a twist transition. On the other hand, one would expect nematic droplets in dispersions of semi-flexible particles to be able to support a twisted director field, because calculations show that  $\gamma_{22} \approx 1/3$  and  $\gamma_{33} \approx 1$  [29, 34, 35]. This is in qualitative agreement with experimental data albeit that the ratio of the twist and splay constant is in practice somewhat lower than predicted,  $\gamma_{22} \approx 0.04 - 0.15$  [33, 34, 36, 37, 38, 39].

The question thus arises why twisted textures have not been observed in lyotropic nematics. To answer this question, we generalize equation (4) to nonspherical, spindle-like droplets, and allow for director-field configurations that are not necessarily truly bipolar. As shall become clear, both finite-size effects and non-sphericity (typical of lyotropic nematic tactoids) conspire against the twisted state.

### 3. Parametrization

Following the prescription of references [8, 9, 10], we impose the geometry of the director field and that of the droplet shape. See figure 2. They are a function of three free parameters, being the aspect ratio of the droplet, the position of the foci of the bispherical director field [8, 9, 40] and the surface twist angle [10]. The director

field is chosen in such a way that it can transform continuously from a homogeneous to a bipolar field and from an untwisted to a twisted one. The droplet shape varies continuously from spherical to spindle like, i.e., elongated with sharp ends. For the given director fields and droplet shapes, discussed in more detail below, we calculate the total free energy, equation (1), and minimize it with respect to the free parameters.

Inspired by the works of Williams [10] and Kaznacheev and co-workers [12, 13], we assume the director field  $\mathbf{n}$  to be twisted bispherical, that is, the director field lines connect virtual point defects [41], situated on the main-body axis of the drop and a distance  $2\tilde{R}$  apart. (See also our previous work [9].) Each director field line lies on a surface of revolution of a circle section about the main axis as shown in Figure 1. Without loss of generality, we assume the latter to coincide with the  $z$ -axis, and the origin to be separated a distance  $\tilde{R}$  from both virtual defects. As for the shape of the droplet, contrary to Williams' assumption, we assume it not to be necessarily spherical but potentially elongated. Its surface is the surface of revolution of a circle section around the  $z$ -axis. This shape very accurately describes the shape of actual tactoids [2, 9, 13]. The distance between the two poles of the droplet is set equal to  $2R$ , where  $R \leq \tilde{R}$ , and the droplet is positioned symmetrically in the director field, that is, both poles are a distance  $R$  away from the origin (see Figure 2). We perform all the calculations in bispherical coordinates  $(\xi, \eta, \phi)$ , because of the symmetry of the problem in hand and because of the fact that a surface of constant  $\eta$  is the surface of revolution of a circle section, see Figure 3. For further details of our parametrization see the Appendix A.

We expect the twist deformation, if there is one, to be small near the line connecting the two poles of the droplet and to grow larger towards the surface of the droplet. The reason for this is that introducing twist near the center of the droplet will greatly increase the amount of bend deformation, whereas introducing it near the surface has a much smaller effect. Hence we expect the angle  $\alpha$  between a director field line and a meridian on the surface of revolution on which the line resides to depend strongly on the  $\eta$ -coordinate but much more weakly on the  $\xi$ -coordinate. As a first approximation, we neglect the dependence on  $\xi$  and assume that  $\alpha = \alpha(\eta)$ . To keep things simple, we furthermore presume  $\alpha$  to only depend on a single parameter, i.e.,  $\alpha(\eta) = \alpha_0 f(\eta)$ , where  $\alpha_0$  sets the maximum twist angle at the surface of a drop and  $f(\eta)$  is some function of  $\eta$ . To fix the latter, we demand that  $\alpha(\eta) \propto \eta^\delta$  if  $\eta \downarrow 0$ , with  $\delta > 0$ . This requirement is needed to keep the contributions from the twist and the bend to the elastic free energy deformation finite, and confirms the earlier claim that near the center of the droplet the twist should be small. Following Williams [10], we use the Ansatz  $\alpha(\eta) = \alpha_0 \sin \eta$  that fulfills all requirements.

Now that we have established our parametrization of the problem, we can find the optimal droplet shape and director-field configuration by minimizing the free energy at a constant volume with respect to the free parameters  $\epsilon$ ,  $\tilde{R}$  and  $\alpha_0$ . Before doing this, we first make the free energy dimensionless by dividing it by  $\tau V^{2/3}$ . The dimensionless

free energy  $\tilde{F}$  then reads

$$\tilde{F} = \frac{F}{\tau V^{2/3}} = \tilde{F}_S + \omega v^{-1/3}(\tilde{F}_{11} + \tilde{F}_{22} + \tilde{F}_{33}), \quad (5)$$

where  $v = V(\tau\omega/K_{11})^3$  is a dimensionless volume, and  $\tilde{F}_S = F_S/\tau V^{2/3}$  and  $\tilde{F}_{ii} = F_{ii}/K_{11}V^{1/3} = \gamma_{ii}I_{ii}/V^{1/3}$  are dimensionless free energies with  $I_{ii} \equiv F_{ii}/K_{ii}$ ;  $F_{ii}$  is the contribution to  $F_E$  associated with the constant  $K_{ii}$ . See the Appendix A. The ratios  $\gamma_{11} \equiv K_{11}/K_{11} = 1$ ,  $\gamma_{22} \equiv K_{22}/K_{11}$  and  $\gamma_{33} \equiv K_{33}/K_{11}$  measure the deviation from the equal constant approximation. Because of the scaling  $F_{ii} \propto V^{1/3}$  and  $F_S \propto V^{2/3}$ ,  $\tilde{F}_{ii}$  and  $\tilde{F}_S$  do not depend on the volume of the droplet, only on its shape and director field. The free energy equation (5) is a function of the free parameters  $\omega$ ,  $v$ ,  $\gamma_{22}$  and  $\gamma_{33}$ .

#### 4. Bipolar drops: analytical results

As already mentioned, Williams' criterion [10] for the onset of the twist transition equation (4) is strictly valid for spherical bipolar droplets only, i.e., in the limit of infinitely large droplets [8, 9]. We extend this result to droplets of finite size. Before turning to the more general case of quasi-bipolar director fields we first allow for non-spherical droplet shapes given a truly bipolar director field, which corresponds to the situation where  $\omega \rightarrow \infty$ . For that case we can analytically calculate a generalization of inequality (4). Note that according to theoretical estimates  $\omega \approx 1$  for lyotropic systems, although experiments point at somewhat larger values closer to ten [8, 9, 13].

Let us assume that the transition from an untwisted to a twisted director field is continuous, that is, the twist angle  $\alpha_0$  changes continuously from zero to a non-zero value, an assumption that will be supported by numerical results discussed below. Near the transition, we can then make a Taylor expansion of the free energy for small  $\alpha_0$ ,

$$\tilde{F} \simeq \tilde{F}\Big|_{\alpha=0} + \frac{\partial \tilde{F}}{\partial \alpha}\Big|_{\alpha=0} \alpha_0 + \frac{1}{2} \frac{\partial^2 \tilde{F}}{\partial \alpha^2}\Big|_{\alpha=0} \alpha_0^2. \quad (6)$$

For symmetry reasons, the first non-constant term in  $\alpha_0$  should be of second order in  $\alpha_0$  so  $\partial \tilde{F}/\partial \alpha = 0$  for  $\alpha = 0$ . At the point where the twist transition occurs, the coefficient of the  $O(\alpha_0^2)$ -term vanishes. This coefficient can be calculated by putting  $R = \tilde{R}$  (the director field being bipolar) and expanding  $(\nabla \cdot \mathbf{n})^2$ ,  $(\mathbf{n} \cdot \nabla \times \mathbf{n})^2$  and  $(\mathbf{n} \times (\nabla \times \mathbf{n}))^2$  in powers of  $\alpha_0$ , and then performing the integrations of equation (A.11). Because the droplet is bipolar, we have  $(\mathbf{n} \cdot \mathbf{q}) = 0$  so the surface term  $F_S$  does not depend on  $\alpha_0$ .

We thus find for the coefficient of the  $O(\alpha_0^2)$ -term

$$\frac{1}{2} \frac{\partial^2 \tilde{F}}{\partial \alpha^2}\Big|_{\alpha=0} = \frac{4\pi\omega R}{v^{1/3}V(\epsilon)^{1/3}(1+\epsilon^2)^2} (-4f_1(\epsilon) + 4f_2(\epsilon)\gamma_{22} + f_3(\epsilon)\gamma_{33}), \quad (7)$$

where the volume  $V(\epsilon)$  is given by equation (A.14), and

$$f_1(\epsilon) = (1 + \epsilon^2)^2 \arctan^2 \epsilon - \epsilon^2, \quad (8)$$

$$f_2(\epsilon) = f_1(\epsilon) + 2\epsilon(1 - \epsilon^2) \arctan \epsilon, \quad (9)$$

$$f_3(\epsilon) = f_1(\epsilon) - 2f_2(\epsilon) + 4\epsilon^2. \quad (10)$$

Bipolar droplets attain a twisted director-field structure, if equation (7) becomes negative, i.e., if

$$f_1(\epsilon) \geq \gamma_{22}f_2(\epsilon) + \frac{1}{4}\gamma_{33}f_3(\epsilon), \quad (11)$$

because then the free energy is unstable to a perturbation away from zero twist angle. Equation (11) is a generalization of the Williams inequality equation (4) for elongated nematic droplets of aspect ratio  $\epsilon$ . Setting  $\epsilon = 1$  in equation (11) reproduces equation (4), as it should. Figure 4 shows a contour plot of the reciprocal aspect ratio  $\epsilon$  as a function of  $\gamma_{22}$  and  $\gamma_{33}$  when the equality in equation (11) holds. For a given value of  $\epsilon$ , droplets of nematic liquid crystal with a combination of elastic constants lying below the contour line corresponding to that value of  $\epsilon$  have a twisted structure, droplets lying above are untwisted. From figure 4, we conclude that when the aspect ratio increases ( $\epsilon$  decreases), there are fewer possible combinations of elastic constants that give a twisted droplet structure, so the larger the aspect ratio, the harder it is to get a twisted structure. Typical values of  $\epsilon$  obtainable from experiments on colloidal dispersion are 0.1 – 0.5 [7, 8, 13].

As it happens, the aspect ratio of a nematic drop is not a free parameter—it sets itself so as to minimize the free energy. For a bipolar droplet with  $\tilde{R} = R$  and  $\alpha(\eta) \equiv 0$  we find that the free energy has the form (see also [8])

$$\tilde{F} = 8\pi(1 + \epsilon^2)c_2(\epsilon)c_3(\epsilon)^2 + 8\pi\omega v^{-1/3}c_3(\epsilon) \left( \left(1 + \frac{3}{4}\gamma_{33}\right) c_2(\epsilon) - \gamma_{33}\epsilon \arctan^2 \epsilon \right), \quad (12)$$

where

$$c_2(\epsilon) = \epsilon - (1 - \epsilon^2) \arctan \epsilon \quad (13)$$

and

$$c_3(\epsilon) = \left(\frac{3}{4\pi}\right)^{1/3} (3(1 + \epsilon^2)^2 c_2(\epsilon) - 4\epsilon^3)^{-1/3}. \quad (14)$$

This free energy is valid all the way to the critical conditions set by equation (11). To find the optimal  $\epsilon$  for a given droplet volume  $v$  and elastic constants  $\gamma_{22}$  and  $\gamma_{33}$ , we simply set  $\partial\tilde{F}/\partial\epsilon = 0$ . This produces an implicit expression for  $\epsilon$  that we do not reproduce here. We have only been able to find an explicit solution if  $v^{1/5}\omega^{-3/5} \lesssim 1$ , in which case  $\epsilon \sim (1/4)(15/8\pi)^{1/5}v^{1/5}\omega^{-3/5} \ll 1$  and the drops are very elongated. For small  $\epsilon$ ,  $f_1(\epsilon) \sim 4\epsilon^4/3$ ,  $f_2(\epsilon) \sim 2\epsilon^2$  and  $f_3(\epsilon) \sim 4\epsilon^4$ , so the parity broken structure only occurs if  $\gamma_{22}$  is very small, i.e., at most  $\epsilon^2$  or smaller than that, unless  $\gamma_{33} \geq 4/3$  in which case the twisted state is absolutely unstable for all  $\gamma_{22}$ . This confirms again that twisted director fields are very unlikely in elongated tactoids.

We note that since  $f_2(\epsilon)/f_1(\epsilon)$  and  $f_3(\epsilon)/f_1(\epsilon)$  are both monotonically decreasing functions of  $\epsilon$ , and since  $\epsilon$  is a monotonically increasing function of the droplet volume [8], that if a twist transition occurs in a bipolar droplet at  $v = v_0$  the droplet must be

twisted for all  $v > v_0$  but untwisted for  $v < v_0$ . Our numerical studies, presented in the next section confirm this.

Returning to the issue whether or not the saddle-splay elastic deformation has any appreciable impact on the twist transition, we find that if we add its contribution

$$- K_{24} \int_V d^3\mathbf{r} \nabla \cdot [\mathbf{n} (\nabla \cdot \mathbf{n}) + \mathbf{n} \times (\nabla \times \mathbf{n})] \quad (15)$$

to the total free energy, the generalized Williams inequality, equation (11), becomes

$$f_1(\epsilon) + \gamma_{24} f_4(\epsilon) \geq \gamma_{22} f_2(\epsilon) + \frac{1}{4} \gamma_{33} f_3(\epsilon). \quad (16)$$

Here  $\gamma_{24} \equiv K_{24}/K_{11}$  and  $f_4(\epsilon) = \epsilon(1 - \epsilon^2) \arctan \epsilon$ . We immediately see that for nearly spherical drops we retrieve the original Williams inequality, (4), because  $f_4(\epsilon) \rightarrow 0$  as  $\epsilon \uparrow 1$ . This implies that the splay-bend contribution is small compared to the other elastic contributions for nearly spherical droplets and that we can indeed neglect it. However, in the opposite limit where the droplet is strongly elongated this is no longer the case. Inserting the limit  $\epsilon \downarrow 0$  in equation (16), our generalized Williams inequality becomes  $\gamma_{24} \geq 2\gamma_{22}$ , showing that the splay-twist elastic term may indeed stabilize the twisted state if the splay-bend elastic constant is sufficiently large. Unfortunately, as far as we are aware, not even an order-of-magnitude estimate is known of  $\gamma_{24}$ , at least not for lyotropic nematics. We can, in spite of this, nonetheless make headway by presuming that the Nehring-Saupe equality [42]  $2\gamma_{24} = 1 - \gamma_{22}$  holds. (See, however, [28].) Presuming it holds, our generalized Williams inequality simplifies to  $\gamma_{22} \leq 1/5$ , indicating that very slender tactoids formed in dispersions of semi-flexible polymers could potentially undergo a parity-breaking transition induced by the splay-bend surface elasticity. We think that this phenomenon is unlikely to be observed in practice, because typically  $\epsilon > 0.1$  [7, 8, 12], i.e., tactoids are in practice just not sufficiently slender. In addition, to become sufficiently slender they would have to be very small, and small tactoids tend to revert to a uniform director field as the calculations presented in the next section show. For these reasons, we think it justified to focus on the bulk elasticity of the droplets.

## 5. General case: numerical results

Now we consider the more general case, where the director field in the droplet is intermediate between uniform and truly bipolar. As we [9], and others [13] recently argued, nematic tactoids are usually only approximately bipolar, with a director field that becomes increasingly uniform the smaller their size. For this more general case it is not possible to analytically derive a further generalization of equation (4). We therefore proceed to investigate the droplet shape and structure using numerical methods. The optimal values for the aspect ratio  $\epsilon$ , degree of curvature of the director field  $\tilde{R}$  and maximum twist angle  $\alpha_0$  are determined by numerically minimizing equation (5) with respect to these quantities at fixed values of  $\omega$ ,  $v$ ,  $\gamma_{22}$  and  $\gamma_{33}$ , using the quasi-Newton algorithm E04JYF from the NAG<sup>®</sup> Fortran Library, release Mark 18.

As already mentioned, the free energy cost of introducing a twist in the director field near the surface of the droplet is less than that in the center. This implies that introducing twist near the surface of a spherical droplet is less costly in terms of free energy than near the surface of an elongated droplet, assuming  $\tilde{R}/R$  is the same for both droplets. We also expect that introducing twist in a bipolar droplet, where there is a lot of splay deformation near the poles, has a larger effect than introducing twist in a droplet of the same shape, but with a more homogeneous director field.

This then leads us to the conjecture that if a transition occurs for a certain value  $v = v_0$  for a given set of fixed values of  $\omega$ ,  $\gamma_{22}$  and  $\gamma_{33}$ , the droplet must be twisted for all  $v > v_0$  but untwisted for  $v < v_0$ . This is true for bipolar droplets as we showed above, but is plausible for the more general case too on account of how the aspect ratio  $\epsilon^{-1}$  depends on  $v$ . (See, again, reference [9].) One of the consequences of this conjecture is that if inequality (4) predicts a droplet to be untwisted, the director field inside the droplet will be untwisted at every volume. The reason is that equation (4) is formally valid only for  $v \rightarrow \infty$ .

The first case we investigate is the so called equal-constant approximation  $\gamma_{22} = \gamma_{33} = 1$ , for which  $K_{11} = K_{22} = K_{33}$ . This combination of elastic constants does not satisfy inequality (4), so, on account of the conjecture we put forward in the previous paragraph, we do not expect a twisted director field in the droplet at any volume. This is indeed what we find from the numerical minimization: for  $\omega = 0.01, 1$  and  $100$ ,  $\alpha_0 = 0$  for all  $v$  tested in the range from  $10^{-18}$  to  $10^{18}$ . Next, we study a combination of elastic constants valid for rod-like colloids. Putting  $\gamma_{22} = 1/3$  in equation (4), we see that for a spherical bipolar droplet to be twisted, we must have  $\gamma_{33} < 1.55$ , which is much lower than the typical value for rod-like colloids of  $\gamma_{33} \gtrsim 5$ . (See section 2.) So, again from the conjecture from the previous paragraph, we do not expect a twisted director field at any droplet volume. This is confirmed for  $\gamma_{33} = 5$  and  $\omega = 0.01, 1$  and  $100$  by a numerical minimization for dimensionless volumes from  $10^{-18}$  to  $10^{18}$ .

Let us now keep the value of  $\gamma_{22}$  fixed at  $1/3$ , but take for  $\gamma_{33}$  a value of  $1$ . Inequality (4) now predicts a twisted director field to be stable in the limit of an infinite volume implying that it might also be stable for some finite volume. That this is indeed the case, is shown in Figure 5, where we show the twist angle  $\alpha_0$  as a function of the dimensionless volume  $v$  for  $\omega = 0.01, 1$  and  $100$ . We see that the transition is sharp and continuous, which was our assumption in deriving the results of section 3. This means that the droplet is absolutely untwisted until the volume reaches the critical size  $v = v_0$ , from whereon the twist gradually increases with increasing  $v$ . For  $\omega = 100$ , the twist transition is not shown, but according to our calculations it occurs at  $^{10}\log v_0 = 10.60$ . This can in fact be checked numerically via a different route. The aspect ratio at the transition can be calculated using the generalized Williams condition equation (11). Because the director field at the transition is nearly bipolar (see figure 6 and the next paragraph), the aspect ratio should also minimize equation (12), which then determines  $v_0$ . We find that  $^{10}\log v_0 = 10.61$  in good agreement with our previous estimate.

In figure 6 we have plotted a diagram of states for  $\gamma_{22} = 1/3$  and  $\gamma_{33} = 1$ . The

twist transition is the only transition in the diagram that is sharp, i.e., on one side of the line demarcating the transition, the droplets are untwisted whereas they are twisted on the other. The line demarcating the transition from a homogeneous to a bispherical director field is drawn at the point where  $\tilde{R} = 2R$ , and one showing the transition in the aspect ratio from spheroidal to elongated is set at  $\epsilon = 1/2$ . Both are smooth crossovers, discussed in more detail in reference [9]. This means that a droplet, e.g., in that part of the phase diagram indicated by "spheroidal twisted bipolar" is not exactly spherical nor exactly bipolar, but nearly so albeit that the director field is indeed twisted.

Figure 6 shows that, at the twist transition,  $v$  is independent of  $\omega$  when  $\omega$  is small, whereas for large values of  $\omega$  this is not so with  $v \sim \omega^3$ . The first result can easily be understood by noting that  $\omega$  describes the degree of anisotropy of the anisotropic surface tension. If  $\omega$  is small, this anisotropy is small and it will not influence the droplet shape nor the director-field configuration. The second observation follows from the fact that when the droplet is bipolar, the aspect ratio must be constant at the twist transition. This can be seen from equation (11), which is independent of  $\omega$ , implicating that the aspect ratio is constant as a function of  $\omega$  if  $\gamma_{22}$  and  $\gamma_{33}$  are constant. We have shown in previous work [9] that if  $\omega \gg 1$ , the aspect ratio  $\epsilon$  of a quasi-bipolar droplet scales as  $v^{-1/5}\omega^{3/5}$ , from which one can conclude that  $v \sim \omega^3$  if  $\epsilon$  is constant and  $\omega \gg 1$ . (See also equation (12).)

Next, we take  $\gamma_{22} = 0.05$  and  $\gamma_{33} = 1$ , which are representative values of the elastic constants for semi-flexible particles (see section 2). In figures 7 and 8, we show the twist angle  $\alpha_0$  as a function of the dimensionless volume  $v$  for anchoring strengths  $\omega = 0.01$ , 1 and 100, and the corresponding diagram of states. The behavior of the droplets is similar as for the previous set of parameter values, except that the twist transition now occurs at a much lower value of  $v$  and that the diagram of states is somewhat more complex. This is to be expected, considering that the twist elastic constant is much smaller. The twist transition for a strong anchoring with  $\omega = 100$  is not shown, but it occurs at  $^{10}\log v_0 = 7.71$ . Using the same method as described earlier in this section we can check this result with the theory of section 4. We find  $^{10}\log v_0 = 7.79$ . The discrepancy between the two results is probably caused by the fact that the droplet is not quite bipolar yet (see figure 8).

As already mentioned, we expect  $\omega \approx 1$  to be a reasonable estimate for the dimensionless anchoring strength. (See again, however, [8, 9, 13].) Because the elastic constants and their ratios differ from system to system, we show, in Figure 9, the dimensionless volume  $v_0$  at which the twist transition occurs for various values of  $\gamma_{22}$  and  $\gamma_{33}$  at a fixed anchoring strength  $\omega = 1$ . As shown in the figure, the larger  $\gamma_{33}$ , the larger the volume of a tactoid needs to be to be able to support a twisted director field. The reason is that a twist deformation goes hand in hand with a bend deformation that is penalized more the larger the bend elastic constant  $K_{33}$ . Also, the larger  $\gamma_{22}$ , the larger the elastic free energy penalty associated with a twist deformation, the smaller  $\gamma_{33}$  must be for the twisted director field to be favorable. The shift to higher droplet volumes is, as discussed, linked with the greater ease of a twist deformation the larger

the drop is because large drops are more spherical than small ones. It is useful to point out that provided the values of the elastic constants and the surface tension are known, figure 9 can be used to estimate the minimum droplet volume at which a transition to a twisted structure should be expected to occur.

We again turn to the question why twisted nematic droplets have so far evaded observation in lyotropic liquid crystals whereas they have been observed in thermotropic ones [5, 24]. We have seen that we should not expect twisted nematic droplets in nematics of hard rods because  $\gamma_{22}$  and  $\gamma_{33}$  are too large. For worm-like, semi-flexible particles such as fd virus though,  $\gamma_{22}$  and  $\gamma_{33}$  possibly have the right values but the volume of the droplets has to be sufficiently large for parity breaking to occur.

In fact, we can use figure 9 to estimate how large. First, we know that  $v \propto V\tau^3$ . Since the elastic constants of a thermotropic and a lyotropic crystal are of the same order of magnitude, we expect the twist transition to occur at about the same value of  $v$ . However,  $\tau$  is typically one or two orders of magnitude larger in a thermotropic liquid crystal than in a lyotropic one [11, 43, 44, 45, 46, 47, 48, 49, 50]. This, then, means that the volume of a droplet of lyotropic liquid crystal at the twist transition must be three to six orders of magnitude larger than that of a thermotropic liquid crystal.

To make our estimate more concrete, we set  $K_{33}/K_{11} = 1$ ,  $K_{22}/K_{11} = 0.05$  and  $\omega = 1$ , and read off from figure 9 that the twist transition occurs if  $v_0 = V(\tau\omega/K_{11})^3 = 10^{1.35}$ . Inserting the typical values  $K_{11} = 10^{-11}$  N and  $\tau = 10^{-6}$  N/m, this corresponds to a droplet volume of  $V \approx 10^4 \mu\text{m}^3$ , with a linear size of about  $30 \mu\text{m}$ . However, if  $\omega$  is closer to 10, as might well be the case [8, 9, 13], this value increases to  $> 300 \mu\text{m}$ . A similar enhancement occurs if  $\tau$  is larger by a factor of ten.

## 6. Conclusion

By adopting a twisted director field structure, a nematic tactoid reduces its splay energy albeit at the expense of increasing its bend and twist energy. Hence, if the bend and twist elastic constants are small enough in comparison to the splay elastic constant, this twisted (parity-broken) structure is energetically more favorable. For a spherical bipolar droplet, Williams [10] derived a criterion, equation (4), the elastic constants have to obey in order to be able to support a twisted director field. In this work we generalized this criterion to bipolar droplets of arbitrary aspect ratio, equation (11), showing that the more elongated the drop the less likely they are to have a twisted director field.

We find the transition to a twisted structure to be sharp, in contrast to the transformation from a uniform director field to a bipolar one. When the transition occurs at a certain dimensionless droplet volume  $v = v_0$ , the droplet is twisted for all  $v > v_0$  but untwisted for  $v < v_0$ . One of the consequences is that droplets that do not have a twisted structure at infinite volume (the limit in which Williams' result is valid), cannot have a twisted structure for any finite volume either. Not entirely surprisingly,  $v_0$  increases with increasing  $\gamma_{33} \equiv K_{33}/K_{11}$  and decreases with increasing  $\gamma_{22} \equiv K_{22}/K_{11}$ .

Nematics of rod-like colloidal particles appear to have elastic constants that do not obey the Williams inequality, so we do not expect to find droplets with a twisted structure in this sort of system. This is not so for dispersions of semi-flexible colloidal particles (or polymers), however, but the tactoids have to be large enough for the twisted director-field configurations to become stable. This is in part due to them becoming less elongated with increasing size.

## Acknowledgments

We are grateful to P. Teixeira for drawing our attention to reference [28].

## Appendix A

The bispherical coordinates are related to the Cartesian coordinates  $\mathbf{x} = (x, y, z)$ , through the relations

$$\begin{cases} x = RZ^{-1} \sin \eta \sin \xi \cos \phi, \\ y = -RZ^{-1} \sin \eta \sin \xi \sin \phi, \\ z = RZ^{-1} \cos \xi, \end{cases} \quad (\text{A.1})$$

where  $Z = 1 + \sin \xi \cos \eta$  and  $0 \leq \xi \leq \pi$ ,  $0 \leq \eta \leq \pi$  and  $0 \leq \phi < 2\pi$ . The Cartesian unit vectors  $\mathbf{e}_x$ ,  $\mathbf{e}_y$  and  $\mathbf{e}_z$  are related to the bispherical unit vectors  $\mathbf{e}_\xi$ ,  $\mathbf{e}_\eta$  and  $\mathbf{e}_\phi$  by

$$\begin{cases} \mathbf{e}_x = Z^{-1} \sin \eta \cos \xi \cos \phi \mathbf{e}_\xi + Z^{-1} (\sin \xi + \cos \eta) \cos \phi \mathbf{e}_\eta - \sin \phi \mathbf{e}_\phi, \\ \mathbf{e}_y = -Z^{-1} \sin \eta \cos \xi \sin \phi \mathbf{e}_\xi - Z^{-1} (\sin \xi + \cos \eta) \sin \phi \mathbf{e}_\eta - \cos \phi \mathbf{e}_\phi, \\ \mathbf{e}_z = -Z^{-1} (\sin \xi + \cos \eta) \mathbf{e}_\xi + Z^{-1} \sin \eta \cos \xi \mathbf{e}_\eta. \end{cases} \quad (\text{A.2})$$

Finally,  $h_\xi = |\partial \mathbf{x} / \partial \xi| = RZ^{-1}$ ,  $h_\eta = |\partial \mathbf{x} / \partial \eta| = RZ^{-1} \sin \xi$  and  $h_\phi = |\partial \mathbf{x} / \partial \phi| = RZ^{-1} \sin \xi \sin \eta$  are the metric components of the bispherical coordinate system.

The director field  $\mathbf{n}$  is given by

$$\mathbf{n}(\xi, \eta, \phi) = -\frac{d_2}{\sqrt{d_1^2 + d_2^2}} \cos \alpha(\eta) \mathbf{e}_\xi + \frac{d_1}{\sqrt{d_1^2 + d_2^2}} \cos \alpha(\eta) \mathbf{e}_\eta + \sin \alpha(\eta) \mathbf{e}_\phi, \quad (\text{A.3})$$

where

$$d_1 = (\tilde{R}^2 - R^2) Z \sin \eta \cos \xi, \quad (\text{A.4})$$

and

$$d_2 = (\tilde{R}^2 - R^2) Z \cos \eta + (\tilde{R}^2 + R^2) Z \sin \xi. \quad (\text{A.5})$$

This choice of director field leads to the following expression for the various components of the elastic free energy, equation (2),

$$\nabla \cdot \mathbf{n} = \frac{Z}{\sqrt{d_1^2 + d_2^2}} (4 \cos \xi \cos \alpha + d_1 \alpha_\eta \sin \alpha), \quad (\text{A.6})$$

$$\mathbf{n} \cdot \nabla \times \mathbf{n} = \frac{-Z}{\sin \xi \sqrt{d_1^2 + d_2^2}} \left( \frac{\sin 2\alpha}{\sin \eta} Z \left( \frac{\tilde{R}^2 + 1}{2} Z - 1 \right) + d_2 \alpha_\eta \right), \quad (\text{A.7})$$

$$(\mathbf{n} \times (\nabla \times \mathbf{n}))_\xi = \cot \xi \sin^2 \alpha + \frac{Z d_1 \cos \alpha}{\sin \xi (d_1^2 + d_2^2)} (2 \sin^2 \xi \sin \eta \cos \alpha - d_2 \alpha_\eta \sin \alpha), \quad (\text{A.8})$$

$$(\mathbf{n} \times (\nabla \times \mathbf{n}))_\eta = \frac{\sin^2 \alpha (\sin \xi + \cos \eta)}{\sin \xi \sin \eta} + \frac{d_1^2 Z \alpha_\eta \sin 2\alpha}{2 \sin \xi (d_1^2 + d_2^2)} + \frac{2 d_2 Z \sin \xi \sin \eta \cos^2 \alpha}{d_1^2 + d_2^2}, \quad (\text{A.9})$$

and

$$(\mathbf{n} \times (\nabla \times \mathbf{n}))_\phi = \frac{-\cos \alpha}{\sqrt{d_1^2 + d_2^2}} \left( \frac{d_1 \sin \alpha (\sin \xi + \cos \eta)}{\sin \xi \sin \eta} + \frac{d_1 Z \alpha_\eta \cos \alpha}{\sin \xi} - d_2 \cot \xi \sin \alpha \right), \quad (\text{A.10})$$

where  $\alpha_\eta = d\alpha(\eta)/d\eta$  and  $(\mathbf{n} \times (\nabla \times \mathbf{n}))_i$  denotes the component of  $\mathbf{n} \times (\nabla \times \mathbf{n})$  in the  $i$ -direction, where  $i \in \{\xi, \eta, \phi\}$ .

Within the bipolar coordinate system, the surface of a droplet with aspect ratio  $\epsilon^{-1}$  is given by  $\eta = \eta_0 = 2 \arctan \epsilon$ ,  $0 \leq \xi \leq \pi$  and  $0 \leq \phi < 2\pi$ . So, using equations (A.6) – (A.10), we can calculate the splay, twist and bend contributions  $F_{11} \equiv K_{11} I_{11}$ ,  $F_{22} \equiv K_{22} I_{22}$  and  $F_{33} \equiv K_{33} I_{33}$  to the Frank elastic energy,  $F_E = F_{11} + F_{22} + F_{33}$  of equation (2), where

$$\begin{aligned} I_{11} &= \frac{1}{2} \int_V d^3 \mathbf{r} (\nabla \cdot \mathbf{n})^2 = \frac{1}{2} \int_0^\pi d\eta \int_0^{\eta_0} d\xi \int_0^{2\pi} d\phi h_\xi h_\eta h_\phi (\nabla \cdot \mathbf{n})^2, \\ I_{22} &= \frac{1}{2} \int_V d^3 \mathbf{r} (\mathbf{n} \cdot \nabla \times \mathbf{n})^2 = \frac{1}{2} \int_0^\pi d\eta \int_0^{\eta_0} d\xi \int_0^{2\pi} d\phi h_\xi h_\eta h_\phi (\mathbf{n} \cdot \nabla \times \mathbf{n})^2, \\ I_{33} &= \frac{1}{2} \int_V d^3 \mathbf{r} (\mathbf{n} \times (\nabla \times \mathbf{n}))^2 = \frac{1}{2} \int_0^\pi d\eta \int_0^{\eta_0} d\xi \int_0^{2\pi} d\phi h_\xi h_\eta h_\phi (\mathbf{n} \times (\nabla \times \mathbf{n}))^2. \end{aligned} \quad (\text{A.11})$$

The surface free energy becomes

$$F_S = \tau \int_S d^2 \mathbf{r} (1 + \omega(\mathbf{n} \cdot \mathbf{q})^2) = \tau \int_0^\pi d\xi \int_0^{2\pi} d\phi (1 + \omega(\mathbf{n} \cdot \mathbf{q})^2) h_\xi h_\phi |_{\eta=\eta_0}, \quad (\text{A.12})$$

with, for our choice of director field and droplet surface,

$$(\mathbf{n} \cdot \mathbf{q})^2 = \frac{d_1^2}{d_1^2 + d_2^2} \cos^2 \alpha. \quad (\text{A.13})$$

For the volume  $V$  and the surface area  $S$  of the droplet we find

$$V(\epsilon) = \int_0^\pi d\eta \int_0^{\eta_0} d\xi \int_0^{2\pi} d\phi h_\xi h_\eta h_\phi = \frac{\pi}{6} R^3 \left[ 3 \left( \frac{1 + \epsilon^2}{\epsilon} \right)^2 \left( 1 - \frac{1 - \epsilon^2}{\epsilon} \arctan \epsilon \right) - 4 \right] \quad (\text{A.14})$$

and

$$S(\epsilon) = \int_0^\pi d\xi \int_0^{2\pi} d\phi h_\xi h_\phi |_{\eta=\eta_0} = 2\pi R^2 \frac{1 + \epsilon^2}{\epsilon} \left[ 1 - \frac{1 - \epsilon^2}{\epsilon} \arctan \epsilon \right]. \quad (\text{A.15})$$

## References

- [1] Bernal J D and Fankuchen I 1941 *J. Gen. Physiol.* **25** 111
- [2] Zocher H and Török C 1960 *Kolloid Z.* **170** 140
- [3] Bernal J D and Fankuchen I 1937 *Nature* **139** 923
- [4] Dogic Z and Fraden S 2001 *Phil. Trans. R. Soc. Lond. A* **359** 997

- [5] Drzaic P S 1999 *Liquid Crystals* **26** 623
- [6] Drzaic P S 1995 *Liquid Crystal Dispersions* (Singapore: World Scientific)
- [7] Sonin A S 1998 *Colloid J.* **60** 129
- [8] Prinsen P and van der Schoot P 2003 *Phys. Rev. E* **68** 021701
- [9] Prinsen P and van der Schoot P 2004 *Eur. Phys. J. E* **13** 35
- [10] Williams R D 1986 *J. Phys. A: Math. Gen.* **19** 3211
- [11] Williams R D 1976 *Mol. Cryst. Liq. Cryst.* **35** 349
- [12] Kaznacheev A V, Bogdanov M M and Taraskin S A 2002 *JETP* **95** 57
- [13] Kaznacheev A V, Bogdanov M M and Sonin A S 2003 *JETP* **97** 1159
- [14] Virga E G 1994 *Variational Theories for Liquid Crystals* (London: Chapman & Hall)
- [15] Chandrasekhar S 1966 *Molecular Crystals* **2** 71
- [16] Bates M A 2003 *Chem. Phys. Lett.* **368** 87
- [17] Lishchuk S V, Care C M and Halliday I 2004 *J. Phys.: Cond. Mat.* **16** s1931
- [18] Lishchuk S V and Care C M 2004 *Phys. Rev. E* **70** 011702
- [19] Ambrožič M, Formoso P, Goleme A and Žumer S 1997 *Phys. Rev. E* **56** 1825
- [20] Rüdinger A and Stark H 1999 *Liq. Cryst.* **26** 753
- [21] Pergamenschik V M 1993 *Phys. Rev. E* **47** 1881
- [22] Pergamenschik V M 2000 *Phys. Rev. E* **61** 3936
- [23] Kiselev A D 2004 *Phys. Rev. E* **69** 041701
- [24] Volovik G E and Lavrentovich O D 1984 *Sov. Phys.-JETP* **58** 1159
- [25] Kurik M V and Lavrentovich O D 1982 *JETP Letters* **35** 444
- [26] Rapini A and Papoular M J 1969 *Journal de Physique (Paris)* Colloque **30** C4-54
- [27] Polak R D, Crawford G P, Kostival B C, Doane J W and Žumer S 1994 *Phys. Rev. E* **49** R978
- [28] Yokoyama H 1997 *Phys. Rev. E* **55** 2938
- [29] Vroege G J and Odijk T 1987 *J. Chem. Phys.* **87** 4223
- [30] Lee S D and Meyer R B 1986 *J. Chem. Phys.* **84** 3443
- [31] Hurd A J, Fraden S, Lonberg F and Meyer R B 1985 *Journal de Physique (Paris)* **46** 905
- [32] Fraden S, Hurd A J, Meyer R B, Cahoon M and Caspar D L D 1985 *J. de Phys. (Paris)* Colloque **46** C3-85
- [33] Lee S D and Meyer R B 1988 *Phys. Rev. Letters* **61** 2217
- [34] Sato T and Teramoto A 1996 *Macromolecules* **29** 4107
- [35] Odijk T 1986 *Liquid Crystals* **1** 553
- [36] Itou S, Tozaki K and Komatsu N 1991 *Jap. J. Appl. Phys.* **30** 1230
- [37] Taratuta V G, Lonberg F and Meyer R B 1988 *Phys. Rev. A* **37** 1831
- [38] Taratuta V G, Hurd A J and Meyer R B 1985 *Phys. Rev. Letters* **55** 246
- [39] Dupré D B and Duke R W 1975 *J. Chem. Phys.* **63** 143
- [40] The extrapolated bispherical director field is exact for spherical geometries in two spatial dimensions [41]. We thank prof. Rick van Bijnen (TU Eindhoven) for pointing this out to us.
- [41] Rudnick J and Bruinsma R 1995 *Phys. Rev. Lett.* **74** 2491
- [42] Nehring J and Saupe A 1971 *J. Chem. Phys.* **54** 337
- [43] Chen Z Y and Noolandi J 1992 *Phys. Rev. A* **45** 2389
- [44] Cui S M, Akcakir O and Chen Z Y 1995 *Phys. Rev. E* **51** 4548
- [45] van der Schoot P 1999 *J. Phys. Chem. B* **103** 8804
- [46] Langevin D and Bouchiat M A 1973 *Mol. Cryst. Liq. Cryst.* **22** 317
- [47] Chen W, Sato T and Teramoto A 1996 *Macromolecules* **29** 4283
- [48] Chen W, Sato T and Teramoto A 1998 *Macromolecules* **31** 6506
- [49] Chen W, Sato T and Teramoto A 1999 *Macromolecules* **32** 1549
- [50] Chen W and Gray D G 2002 *Langmuir* **18** 633

## Figure Captions

**Figure 1.** Sketch of a twisted director-field line in a spindle-like nematic droplet or tactoid. The twist is largest near the surface of the drop. Close to the center line of the drop the twist is presumably negligible.

**Figure 2.** Droplet surface (thick lines) and defining surfaces for the director field lines (thin lines). The system is rotationally symmetric around the line connecting the two (virtual) defects given by the crossing or focal points of the director field lines.  $R$  is half the length of the major axis of the droplet.  $\tilde{R}$  is half the distance between the virtual defects.

**Figure 3.** The bispherical coordinate system. The unit vector  $\mathbf{e}_\phi$  points out of the plane on the right hand side of the line indicated by  $\eta = 0$ . The picture should be rotated along the line  $\eta = 0$  to get the full three dimensional coordinate system. See the main text for an explanation of the symbols.

**Figure 4.** Contour plot of the inverse of the aspect ratio  $\epsilon$  of a tactoid exactly at the twist transition as a function of the ratios  $\gamma_{33} = K_{33}/K_{11}$  and  $\gamma_{22} = K_{22}/K_{11}$  for bipolar droplets where  $K_{33}$ ,  $K_{22}$  and  $K_{11}$  are the usual bend, twist and splay elastic constants. The numbers next to the contour lines denote the values of  $\epsilon$ . A bipolar droplet has a twisted structure if and only if the point denoting the combination of the ratios of elastic constants  $\gamma_{22}$  and  $\gamma_{33}$  of the nematic lies below the contour line corresponding to the aspect ratio of the droplet.

**Figure 5.** The maximum (surface) twist angle  $\alpha_0$  as a function of the dimensionless volume  $v$  in units of  $\pi$  radians for the ratios of the elastic constants  $\gamma_{33} = K_{33}/K_{11} = 1$  and  $\gamma_{22} = K_{22}/K_{11} = 1/3$  at three different values of the anchoring strength  $\omega$ . For  $\omega = 100$ , the twist transition occurs at  $^{10}\log v = 10.60$  (not shown).

**Figure 6.** The diagram of states for  $\gamma_{33} = K_{33}/K_{11} = 1$  and  $\gamma_{22} = K_{22}/K_{11} = 1/3$ . The diagram shows the shape of the droplet as a function of the dimensionless volume  $v$  and the anchoring strength  $\omega$ . Indicated are the transition from a uniform director field to a bipolar one (vertical line), the transition from a spheroidal to an elongated shape (horizontal line) and the transition from a bipolar to a twisted director field (line in the lower right corner). Only the latter transition is sharp, the transition from uniform to bipolar is (arbitrarily) taken at the boojum position  $\tilde{R}/R = 2$  and the transition from spheroidal to bipolar at an aspect ratio of 2.

**Figure 7.** The twist angle  $\alpha_0$  as a function of the dimensionless volume  $v$  in units of  $\pi$  radians for  $\gamma_{33} = K_{33}/K_{11} = 1$  and  $\gamma_{22} = K_{22}/K_{11} = 0.05$  at three different values of the anchoring strength  $\omega$ . For  $\omega = 100$ , the twist transition occurs at  $^{10}\log v = 7.71$  (not shown).

**Figure 8.** As figure 6, but now with  $\gamma_{33} = K_{33}/K_{11} = 1$  and  $\gamma_{22} = K_{22}/K_{11} = 0.05$ . The various director-field patterns and droplet shapes are again indicated. Notice the increased number of regimes.

**Figure 9.** The value of  $v$  at which the twist transition occurs as a function of  $\gamma_{33}$  for various values of  $\gamma_{22} \equiv K_{22}/K_{11}$  and with  $\omega = 1$ . For given  $\gamma_{22}$ , the droplets above the line have an untwisted structure, whereas the droplets below it have a twisted structure. By adopting a twisted structure, a droplet decreases its splay energy, at the same time increasing its twist and bend energy. For that reason, the twisted structure occurs only if  $\gamma_{33} \equiv K_{33}/K_{11}$  is small enough, even when  $\gamma_{22} = 0$ .

## Figures

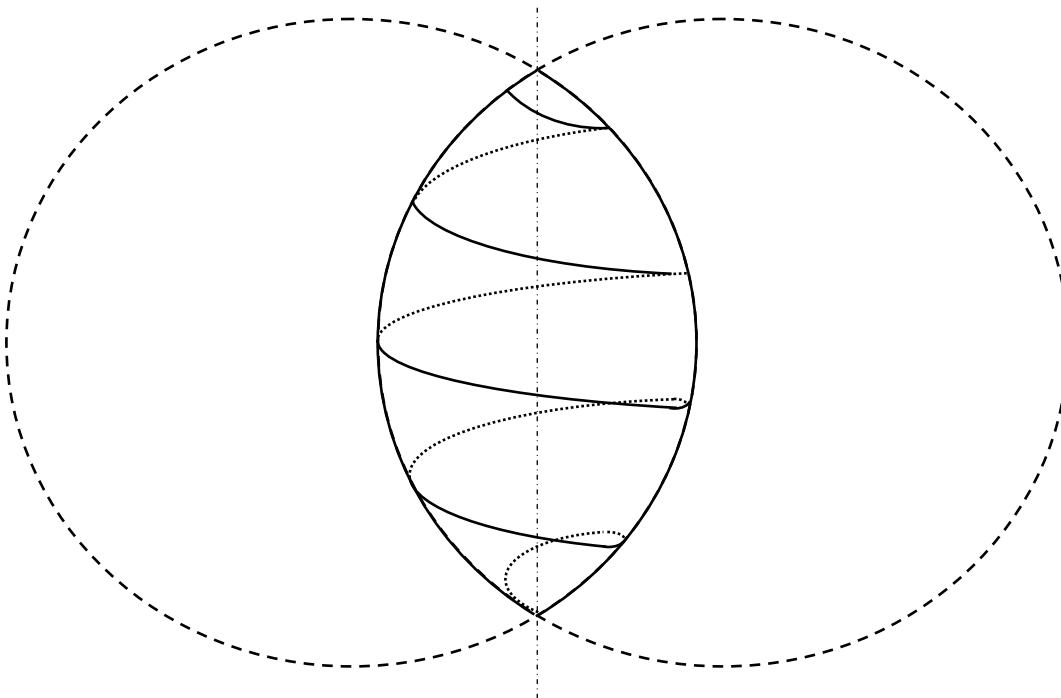


Fig. 1 – Prinsen & Van der Schoot

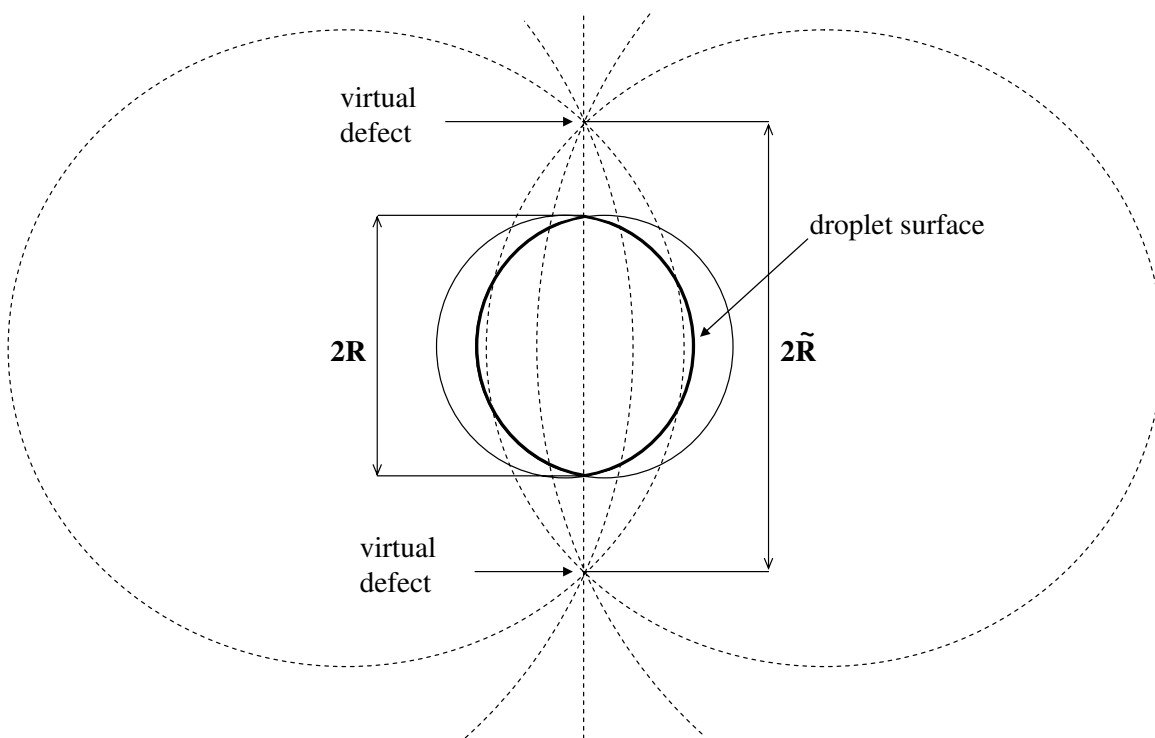


Fig. 2 – Prinsen & Van der Schoot

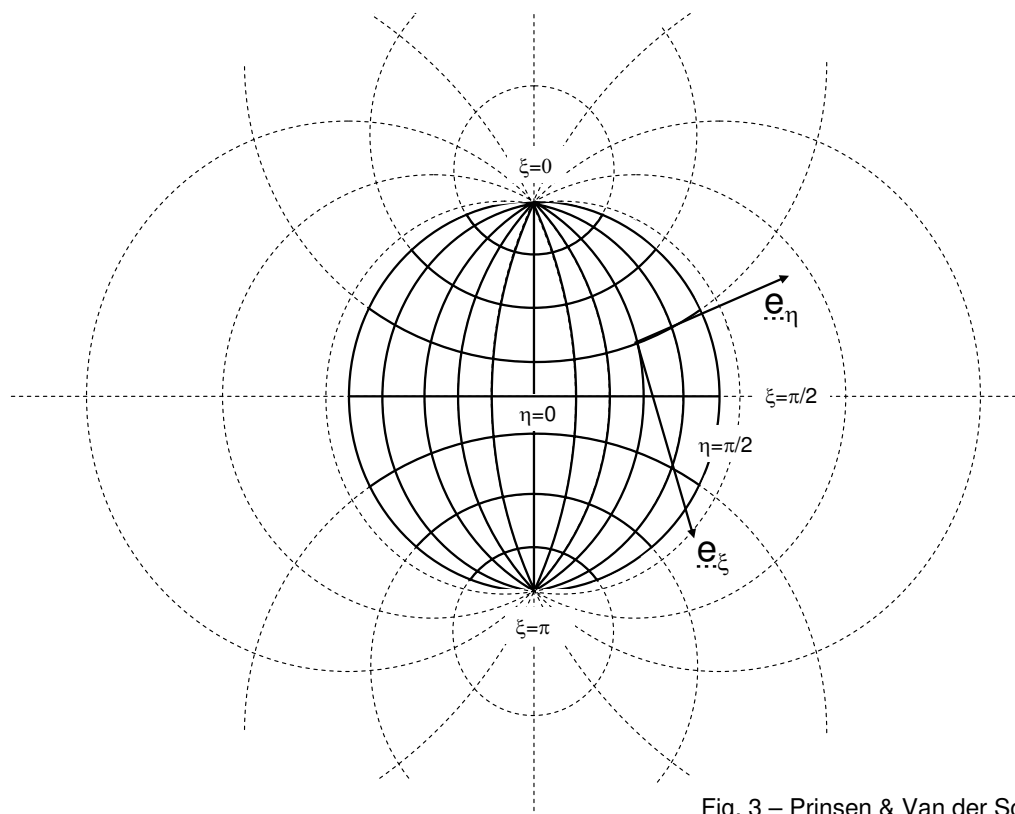


Fig. 3 – Prinsen & Van der Schoot

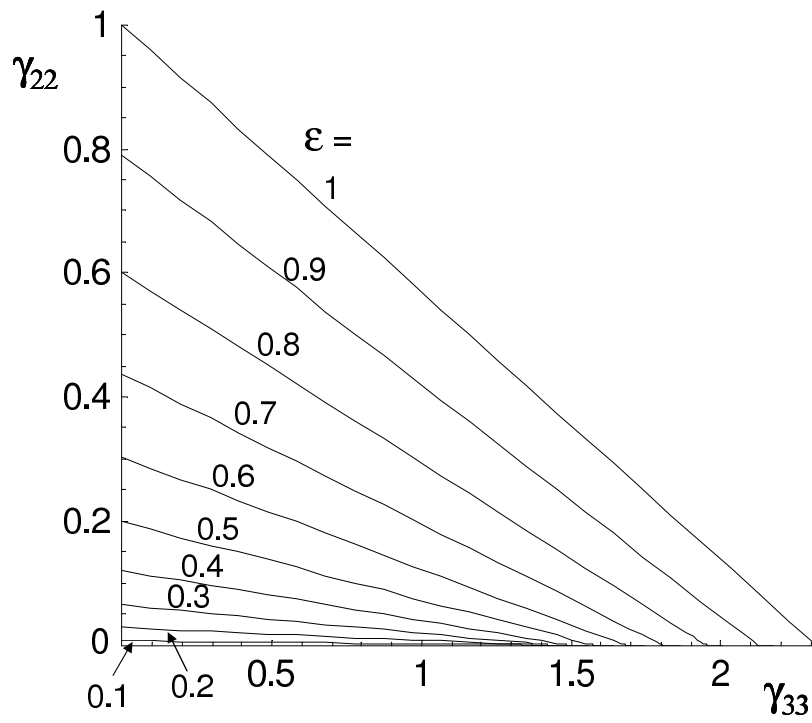


Fig. 4 – Prinsen &amp; Van der Schoot

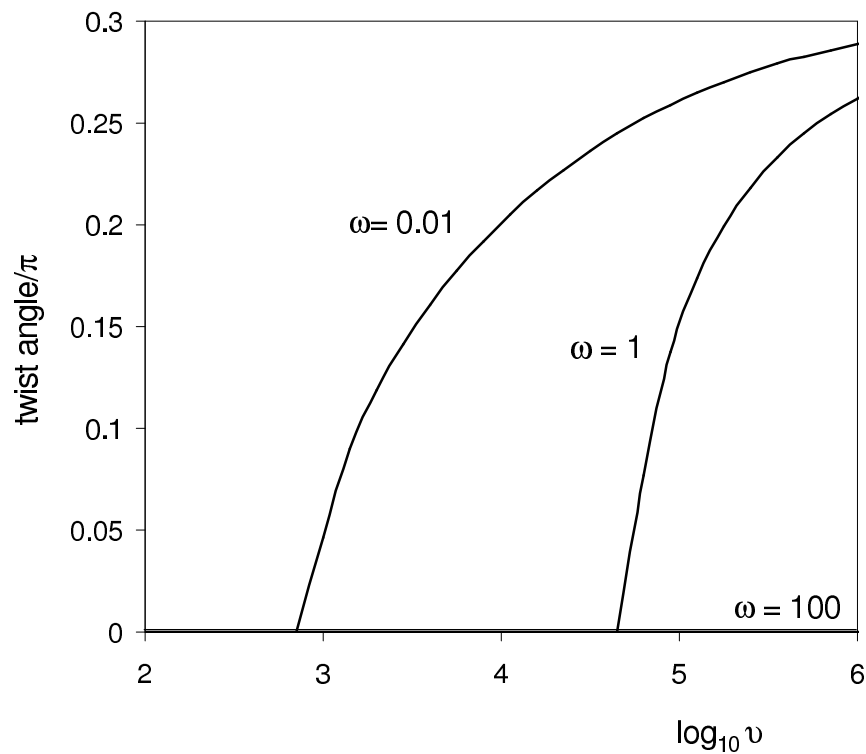


Fig. 5 – Prinsen &amp; Van der Schoot

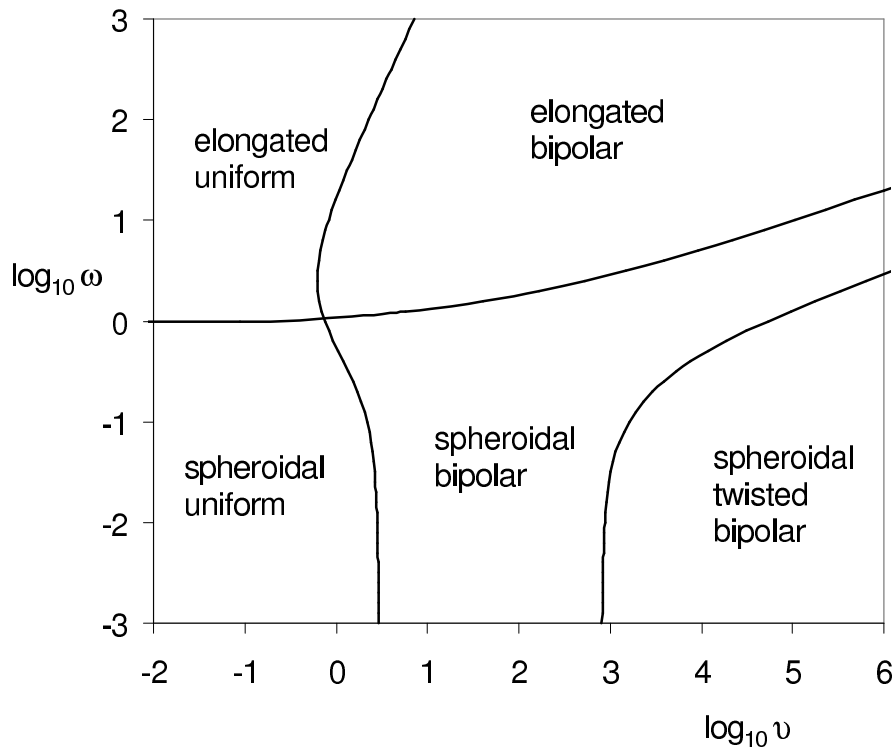


Fig. 6 – Prinsen &amp; Van der Schoot

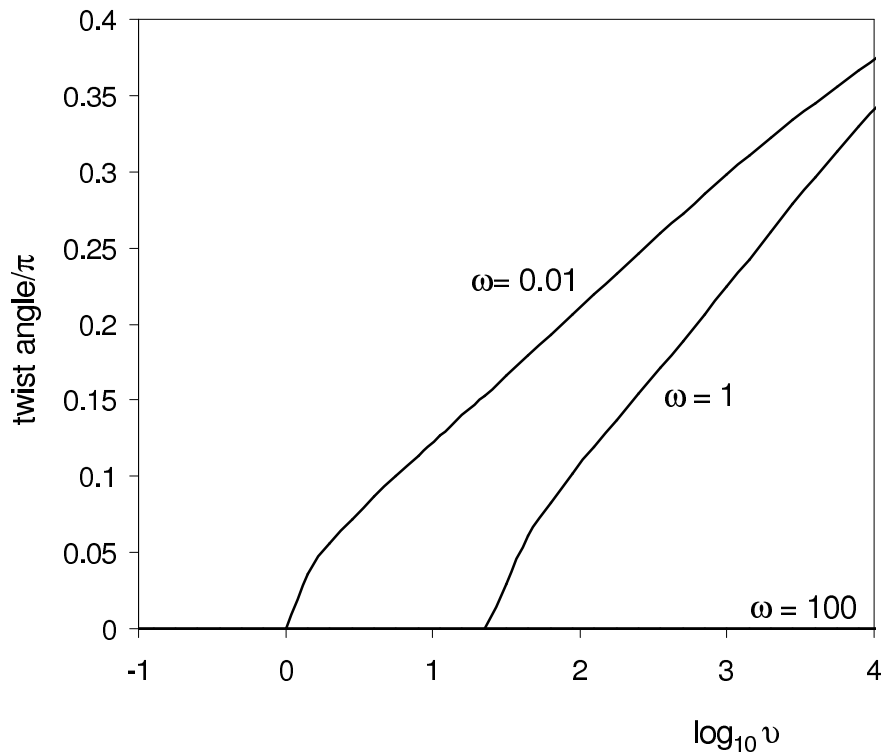


Fig. 7 – Prinsen &amp; Van der Schoot

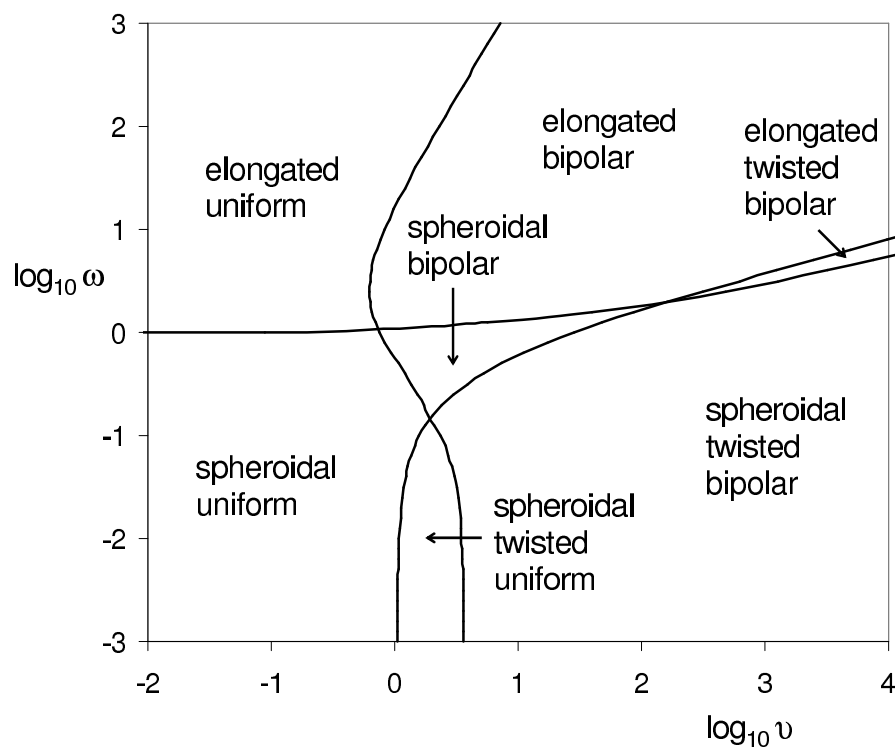


Fig. 8 – Prinsen &amp; Van der Schoot

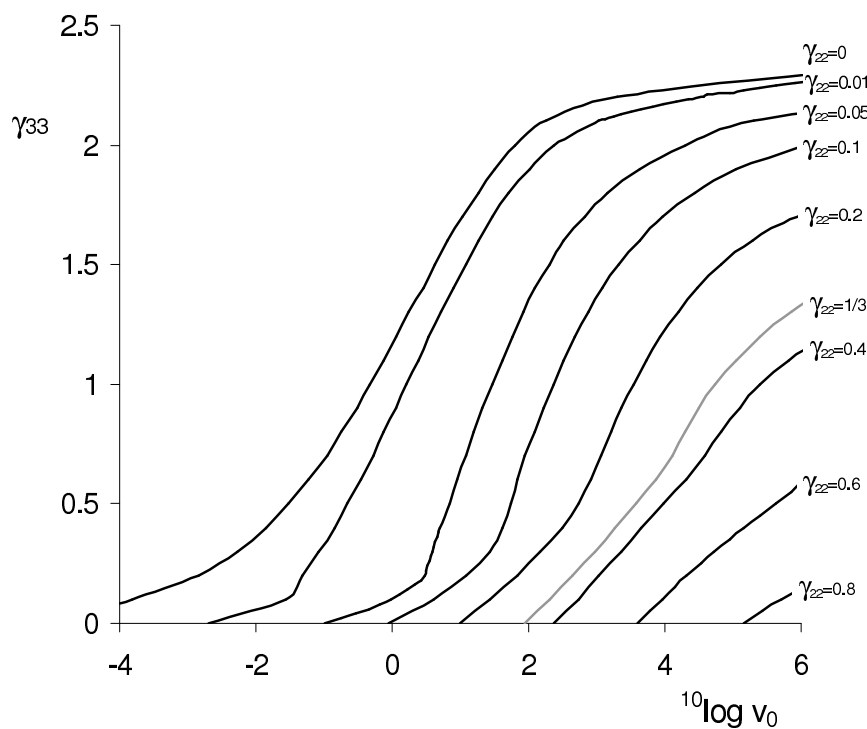


Fig. 9 – Prinsen &amp; Van der Schoot